HEFAT2012
9th International Conference on Heat Transfer, Fluid Mechanics and Thermodynamics
16 – 18 July 2012
Malta

THERMO-HYDRAULIC COMPARISON OF 10 PPI METAL FOAM AND LOUVERED FINS FOR LOW VELOCITY APPLICATIONS

De Schampheleire S.[1,*], De Jaeger P.[1,2], Huisseune H.[1], Ameel B.[1], T'Joen C.[1], De Paepe M.[1]
*Author for correspondence
[1] Ghent University, Department of Heat, Mass and Combustion Mechanics,
Sint-Pietersnieuwstraat 41, 9000 Ghent, Belgium
[2] NV Bekaert SA, Bekaertstraat 2, 8550 Zwevegem, Belgium
E-mail: Sven.DeSchampheleire@ugent.be

ABSTRACT

To maximize the effectiveness and thus minimize the airside resistance, a relatively new heat enhancing material, aluminium foam, is compared with the current state-of-the-art, louvered fins, in a wind tunnel experiment. The comparison between both heat exchangers is done based on a well-defined Performance Evaluation Criterion (PEC), taking heat transfer and pressure drop in account. Furthermore, as the studied heat exchangers are so-called 'low-capacity' units, a non-uniform temperature field downstream the heat exchanger is induced. Therefore an area-mean temperature reading has been developed, with the aid of an infra red camera. Finally, the contribution of the contact resistance to the overall thermal resistance of these pressed-fit heat exchangers is investigated.

INTRODUCTION

Worldwide energy use is continuously increasing. On average, low velocity HVAC applications constitutes 30% of the total energy use in society [1], providing huge potential for energy reduction. One of the most important parts in a HVAC installation is the heat exchanger. Optimizing its effectiveness is of great importance for coping with our future energy requirements. In these systems, the airside convective resistance is dominant, representing up to 75-90% of the overall thermal resistance [2]. Therefore, measures have to be taken to decrease this airside resistance, which typically comes down to maximizing the product of the external convection coefficient and the heat transferring surface area. This can be done by increasing the heat transfer surface area and minimizing the formation of thermal boundary layers. Fins have proven to be a very effective solution for this task. In particular, louvered fins are the current state-of-the-art. Other interesting heat transfer enhancing materials are porous media. One type that has drawn much attention in open literature is open-cell metal foam (see Fig. 1). In this study *aluminium* foam is used, because of its high thermal conductivity (k=200 W/mK). The used foams are in-house manufactured, basically by replicating an organic preform (e.g. from polyurethane) via an investment casting process. The organic preform defines the PPI value (Pores Per linear Inch) of the foam. This PPI value serves as a classifying parameter of the foam [3]. It is directly linked to the specific surface area. In this paper the used PPI value is 10.

It is noteworthy to mention that this preform foam is described by the Plateau laws [3], which are known to be the result of surface energy minimisation. The replication of the thickened preform foam results in a quasi-optimal structure, from which various interesting structural and functional properties arise:

- High porosity (>90%)
- Relatively high strength and toughness, giving them structural stability
- Excellent fluid mixing due to tortuous flow paths
- High specific surface area (typical values ranging from 400 to over 1500 m^2/m^3 when uncompressed)
- High gas permeability
- Low weight
- 3D structure (shape-ability)

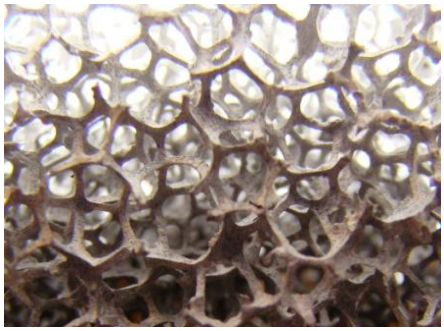

Figure 1 Illustration of the complex shapes in 10 PPI metal foam (in-house manufactured)

The heat transfer potential of foam is compared to conventional techniques (as louvered fins, corrugated ducts, truss cores...) by Lu et al. [4]. When only comparing the Nusselt number (Nu), foam outperforms louvered fins. However, as the good mixing properties heavily disturb the boundary layers, pressure drop is frequently quoted as principal disadvantage. It certainly prevails at high Reynolds numbers.

A commonly used approach in heat transfer engineering is describing all physics by means of a zeroth order model (which is in fact a global-scale analysis method) [5]. This experimental black box method relates kinetic variables (heat transfer, pressure drop) to kinematic variables (temperatures, velocity), by means of proportionality constants (thermal resistance, friction factor). The depending variables which are related via the proportionality constants are averaged, e.g. averaged inlet and outlet temperatures, mean mass flow rate... This technique will also be applied in this paper.

The aim of this paper is a thermo-hydraulic comparison between a state-of-the-art commercial louvered fin-and-tube heat exchanger with a prototype 10 PPI metal foam heat exchanger. By consequence, fouling and economical considerations are not investigated. Such a comparison has been already made by Sertkaya et al. [6] in 2012. However, it is not clear what the uncertainty on the reported data is: mass flow rate is based on local velocity measurement, the thermocouples are not calibrated, the convection coefficient is incorrectly reported and the pressure drop is not according to our measurements (it differs more than a factor 10). Furthermore, this paper provides new insight as thermal contact resistance is taken in account.

NOMENCLATURE

Greek symbols

Δ	$[-]$	difference
δ	$[-]$	uncertainty on
ε	$[-]$	effectiveness in $\varepsilon - NTU$ method (Eq. (10))
η	$[-]$	fin efficiency
μ	$[Pa * s]$	dynamic viscosity
ρ	$[kg/m^3]$	density

Symbols

$\dot{m}$	$[kg/s]$	mass flow
A_c	$[m^2]$	minimal flow area
A_i	$[m^2]$	internal surface area
A_{HX}	$[m^2]$	area section of the heat exchanger (= 0.256x0.447)
A_o	$[m^2]$	heat exchanging surface
A_{ext}	$[m^2]$	external surface area
C_{min}	$[W/K]$	minimal thermal capacity
c_p	$[J/kg\ K]$	specific heat capacity
d_f	$[m]$	strut diameter
f	$[-]$	friction factor (Kays and London)
G_c	$[kg/m^2 s\ ]$	mass flux
h	$[W/m^2K]$	convection coefficient
j	$[-]$	Colburn factor
k	$[W/mK]$	thermal conductivity
L	$[m]$	representative length
LMTD	$[-]$	Logarithmic Mean Temperature Difference
NTU	$[-]$	Number of Transfer Units
Nu	$[-]$	Nusselt number $(= h * \frac{L}{k})$
PEC	[W/K]	Performance Evaluation Criterion
PPI		Pores Per linear Inch
Q	$[W]$	power
R	$[K/W]$	thermal resistance
Re	$[-]$	Reynolds number
R^*_{ext}	$[K/W]$	external convective resistance lumped with the contact resistance, Eq. (12)
$R_{contact}$	$[K/W]$	thermal contact resistance
$R_{overall}$	$[K/W]$	overall thermal resistance
U	$[W/m^2K]$	overall heat transfer coefficient

Subscript

1	inlet
2	outlet
air	airside
i	inside
ext	outside
ref	reference
water	waterside

EXPERIMENTAL SETUP

The experimental set-up consists of an open air wind tunnel and a closed hot water cycle (see Figure 2). A centrifugal fan sucks air through a calibrated nozzle (1). The pressure drop is measured over the nozzle with a differential pressure transducer, with a relative uncertainty of 0.5%. This allows to determine the airside mass flow rate according to the ISO5167 standard. The fan is driven by a frequency controller. The considered range of the airside mass flow rate is between 0.15 and 0.41 kg/s, corresponding with an air speed in the test section of 1.1 to 3.1 m/s. To obtain a uniform velocity profile a diffuser section is used, followed by a settling chamber (with a honeycomb (cell size ½-4 inches long)), a flow straightener and a double sinusoidal contraction section. The uniformity of the inlet airside velocity was confirmed with hotwire measurements. This airside test rig has been tested extensively by T'Joen et al. [7] and Huisseune et al. [8]

To provide heating, a closed water cycle is used. The heater (2) has a maximal power of 9 kW and is PID controlled via a LabVIEW® implementation. The pump (3) has a relay control. A motorized three way valve (4) controls the mass flow rate to the heat exchanger, keeping it below 50% of the maximal flow rate of the pump. By using the water heating system in this way, a very stable temperature can be maintained, as the water circuit acts as a 'hot water buffer' with a large recirculating flow. The water mass flow rate through the heat exchanger is measured by a coriolis mass flow meter (type PROMASS 80-Endhauser, (5)). Based on the calibration sheet, the relative error on the mass flow rate is less than 0.3%. For reference measurements, the water temperature is kept constant at 70°C. This waterside test facility has been used in the PhD thesis of Huisseune [9].

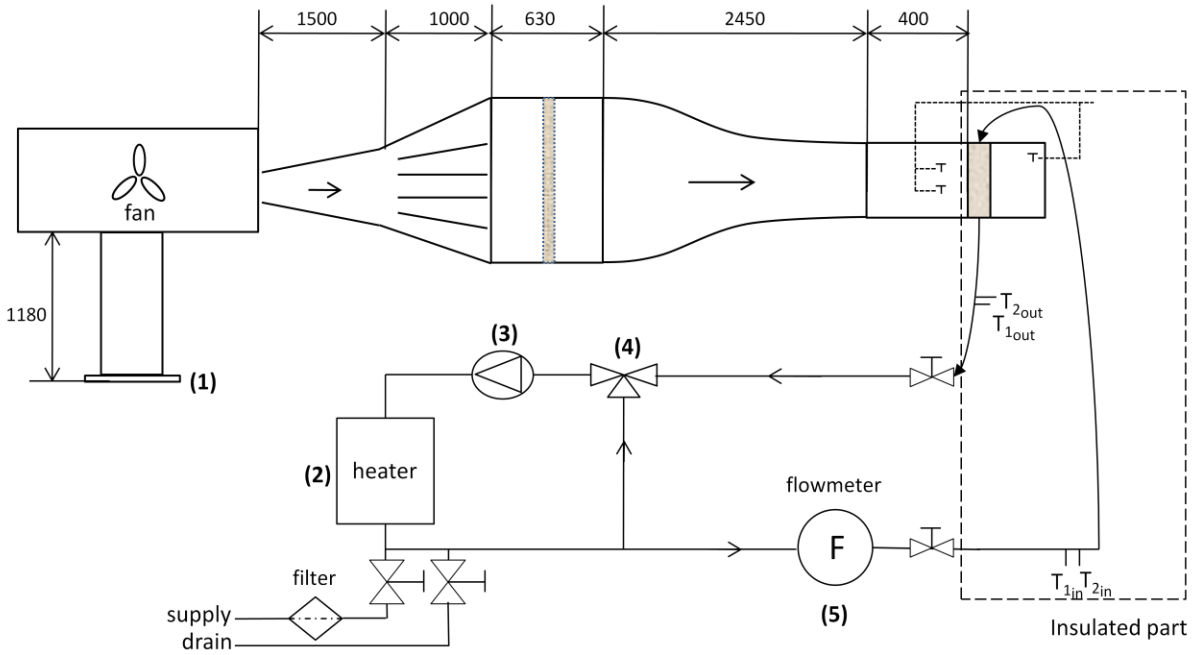

Figure 2 Illustration of experimental setup: wind tunnel (*top*) and water circuit (*below*)

All temperatures are measured with K-type thermocouples (1mm junction diameter), which were calibrated using a temperature calibrator furnace (DBC 150-Druck). The reference temperature is measured with a FLUKE temperature reader (type 1523, with accuracy of 0.015°C). The uncertainty of the thermocouples is ±0.07°C (conservatively taken 0.1°C in the data reduction). The water temperature is measured with four thermocouples, two in the inlet collector and two in the outlet collector.

The airside pressure drop over the heat exchanger is measured with a differential pressure transducer (with a relative accuracy of 0.5%). From the water collectors on, the whole test section is insulated with Eurofloor© insulation (k=0.023 W/mK). Two heat exchangers were tested using this set-up. Both have a cross sectional area of 256x447 mm, a flow depth of 24 mm and two staggered tube rows.

The first heat exchanger (schematically shown in Fig. 3, specifications listed in Table 1) is an off-the-shelf unit with thin aluminium fins. To enhance the heat transfer the fin surface is interrupted. In this case the adapted inclined louvered pattern is used. This design has been studied earlier by T'Joen et al [7]. This heat exchanger is a so-called 'low capacity' unit, which means that not all the tubes are connected to the header. In this case water flows only through 18 of the 24 tubes, as shown in Fig. 3. Although this unit normally is installed at an angle (as can be seen in the figure), it is placed vertically in the wind tunnel, so that both heat exchangers are tested in the same uniform conditions. Measures are taken to prevent bypass flow: by filling the whole surroundings of the heat exchanger with silicones.

The second heat exchanger is in-house manufactured using a 10 PPI aluminium foam with a porosity of 93.73%. The foam is made of pure aluminium (Al1050). The holes, necessary for installing the tubes, are first drilled and then finished using electric discharge machining, to provide a good contact with the copper tubes. The tubes are placed in the holes and are then expanded using an air-pressurized bullet. This press-fit technique is also used for the first heat exchanger.

The tubes of the louvered fin heat exchanger originally have an outside diameter of 7 mm, and are inserted into the 7.2 mm diameter holes in the fins before being expanded. For the metal foam heat exchanger it is chosen to drill holes of 7 mm. When the tubes are then expanded in these holes, the foam is expected to deform, providing a good thermal contact. The external diameter of the expanded tubes is 7.2 mm. The two heat exchangers are shown in Figure 4 for comparison.

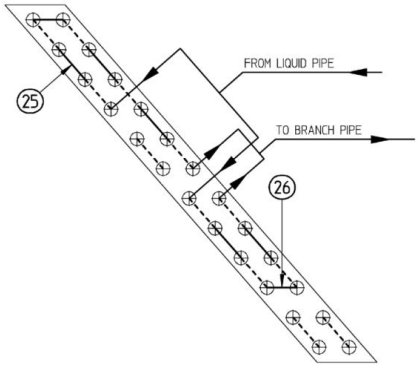

Figure 3 Schematic sketch of the louvered fin heat exchanger

Staggered tube configuration	
Internal diameter	6.66 mm
External diameter	7.2 mm
Fin pitch	1.4 mm
Transversal tube pitch	21 mm
Longitudinal tube pitch	12 mm
Fin thickness	0.115 mm
Depth in airflow direction	24 mm

Table 1 Specifications of the louvered fin heat exchanger

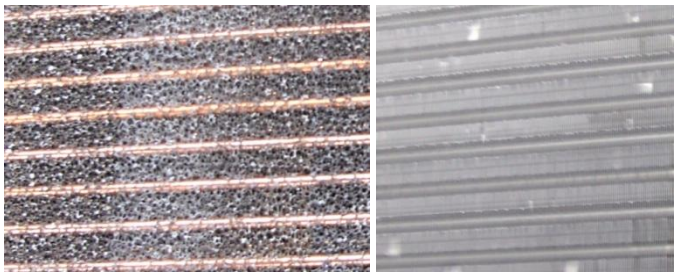

Figure 4 Two studied heat exchangers: metal foam (*on the left*), louvered fins (*on the right*)

PROCEDURE AND DATA REDUCTION

The Wilson plot technique and his different modifications provide a tool for analysing convective heat transfer processes, basically by rewriting the processes with Ohm's law. With the measured inlet and outlet temperature and mean mass flow rate, the heat transfer rate on the air- and waterside can be determined via Eq. (1) and (2).

$$\dot{Q}_{air} = \dot{m}_{air}.c_{p,air}.(T_{air,out} - T_{air,in}) \quad (1)$$

$$\dot{Q}_{water} = \dot{m}_{water}.c_{p,water}.(T_{water,in} - T_{water,out}) \quad (2)$$

According to the ANSI/ASHRAE-33 standard the measurement can be deemed acceptable if the difference between both heat transfer rates is smaller than 5%. For the results in this report, the heat balance closed well within 3% (mostly within 1%). The Wilson plot technique deals with the determination of convection coefficients based on measured experimental data. The technique is based on the separation of the overall thermal resistance into:

(1) convective heat transfer on waterside (inside the tubes) and on airside (R_i and R_{ext})
(2) conductive resistance through the copper tubes (R_{cond})
(3) contact resistance ($R_{contact}$)
(4) fouling resistances ($R_{fouling}$)

$$R_{overall} = \frac{1}{UA} = R_i + R_{cond} + R_{ext} + R_{contact} + R_{fouling}$$
$$= \frac{1}{h_i.A_i} + \frac{\ln\left(\frac{d_{out}}{d_{in}}\right)}{2\pi.k_{tube}.L} + \frac{1}{h_{ext}.A_{ext}.\eta} + R_{contact} + R_{fouling} \quad (3)$$

For this case, the fouling resistance is neglected (a water filter is used). The overall thermal resistance can be calculated with two methods. The first one is the *LMTD* method (Log Mean Temperature Difference), through Eq. (4) and (5).

$$LMTD = \frac{\Delta T_1 - \Delta T_2}{\ln\left(\frac{\Delta T_1}{\Delta T_2}\right)} \quad (4)$$

$$R_{overall} = \frac{F.LMTD}{\dot{Q}_{average}} \quad (5)$$

For the determination of the overall resistance, a correction factor F is needed, which depends on the flow rate ratio and the heat exchanger configuration [5]. In this case, the cross flow configuration was considered resulting in F values ranging between 0.925 and 0.98 (for the two heat exchangers). $\dot{Q}_{average}$ can be determined by combining the data out of Eq. (1) and (2) in a preferred way to minimize the uncertainty. The approach of using a simple average is adopted and promoted widely in heat exchanger community. However, this approach does not minimize the combined absolute uncertainty. This can be done according a procedure described by Park et al. [10]. This way $\dot{Q}_{average}$ and the associated uncertainty are calculated via:

$$\dot{Q}_{average} = \sum_{i=0}^{N} \phi_i \, \dot{Q}_i \quad (6)$$

$$\phi_{water} = \frac{\delta\dot{Q}_{air}^2}{\delta\dot{Q}_{air}^2 + \delta Q_{water}^2} \quad (7)$$

$$\phi_{air} = \frac{\delta\dot{Q}_{water}^2}{\delta\dot{Q}_{air}^2 + \delta\dot{Q}_{water}^2} \quad (8)$$

$$\delta\dot{Q}_{average} = \sqrt{\left(\phi_{air}\,\delta\dot{Q}_{air}\right)^2 + \left(\phi_{water}\,\delta\dot{Q}_{water}\right)^2} \quad (9)$$

The second method to determine the overall thermal resistance is the $\varepsilon - NTU$ method.

$$\varepsilon = \frac{\dot{Q}_{average}}{C_{min}.\Delta T_{max}} \quad (10)$$

C_{min} is the smallest capacitive flow rate of the two fluid streams ($\dot{m}.c_p$). In this study C_{min} is on the airside. Depending on the flow with the smallest capacitive flow rate, NTU is calculated as a function of ε and C^*, which is the ratio of the smallest to the largest capacitive flow rate [5]. In this study, we use the mixed-unmixed heat exchanger model. Eq. (11) represents the thermal overall resistance via the $\varepsilon - NTU$ method.

$$R_{overall} = \frac{1}{C_{min}.NTU} \quad (11)$$

Both methods result in the same overall resistance; however as in [11] the relative uncertainty is minimal for the *LMTD* method. Thus, further use for data reduction is made for this method.

The internal convection coefficient (h_i) in the first term on the *rhs* in Eq. (3) can be determined with the Gnielinski correlation. This correlation is applicable for transitional and turbulent flows ($3000 \leq Re_{internal} = \frac{\rho_{water} * v_{water} * d_{in}}{\mu_{water}} \leq 5 * 10^6$ and $0.5 \leq Pr \leq 2000$), with an assumed uncertainty of 10% for the waterside Nusselt number. All measured data in this paper have internal Reynolds numbers higher than 8500. The friction factor used in this correlation is determined by the recommended Filonenko correlation [5]. The external

convection coefficient (h_{ext}) from the third term on the *rhs* in Eq. (3) is frequently reported as a Nusselt number to compare with literature. However, the exterior surface area of the metal foam (A_{ext}) is needed for this. Several researchers have determined this through a destructive method, with high errors [12]. This results in high uncertainties for the reported Nusselt number and only a limited ability for comparison. Therefore, as proposed by Moffat et al. [13] the parameters h_{ext} and A_{ext} are simply hold as one entity.

Furthermore, for the moment, the external convective resistance and the contact resistance are also taken as one entity (Eq. (12)). In a latter paragraph, R_{ext} and $R_{contact}$ will be decoupled.

$$R^*_{ext} = \frac{1}{h_{ext} \cdot A_{ext} \cdot \eta} + R_{contact} \quad (12)$$

PERFORMANCE EVALUATION CRITERION FOR FOAM

The output of a black box method (thermal resistance and friction factor) can be used to make a comparison between heat exchangers or literature data. A 'good' *Performance Evaluation Criterion* (PEC) is therefore necessary. Defining the performance of a heat exchanger is a complex problem, which depends on a large number of parameters as there is no unique criterion to define the goodness of a heat exchanger. According to Shah [5] there are 16 different PECs. An *area goodness factor*, defined as *j/f*, is commonly applied in metal foam research. It combines heat transfer and pressure drop. T'Joen et al. [11] used a normalized area goodness: $j/j_{ref} * j_{ref}/f$, with reference to plain fins. In their thermo-hydraulic comparison of foam covered and helicoidally finned tubes, the area goodness criterion is associated with the assumption of a fixed pressure drop [5]. As T'Joen refers to plain fins, changes in pressure drop are negligible. In this study however it is not possible to have e.g. a plain fin reference. Additionally, this criterion is less good for metal foams: when a comparison is made between a thick and a thin strut (according to a changing porosity for example), the thinner strut will have a bigger *j/f*, because $h = Nu\ k/d_f$. This makes the heat exchanger more efficient, but because no account of the mantle surface is made, the absolute heat transfer will decrease.

A *volume goodness factor* is a more general approach: the heat transfer surface is plotted against the friction power per unit volume. However, it can only be used in geometries with a same hydraulic diameter. Due to this latter, it cannot be used to compare metal foams with louvered fins.

As can been seen from open literature, for all heat transfer enhancing (fin) materials, heat transfer and fan power ($\dot{m} * \Delta p$) are of importance. The PEC used in this paper is taken as the ratio of *the thermal conductance to the pressure drop* (friction factor), Eq. (13), where f is the Kays and London friction factor (Eq. (14)) and R^*_{ext} is the airside resistance (calculated by Eq. (12)).

$$PEC = \frac{1}{R^*_{ext} * f} \quad (13)$$

$$f = \frac{A_c}{A_0} . \frac{2\ \Delta P\ \rho_{atm}}{G_c^2} \quad (14)$$

MEASUREMENTS

The measurements were performed under steady state condition. To determine whether the unit was in steady state, the setup was operated first over a long time (at least for 2.5 hours), to ensure that the large thermal insulation had reached thermal equilibrium. Next, the variation of the water and air inlet temperature was monitored. Once this variation was below 0.07°C during 200s, the measurements could start. All measurements at different temperature set points were performed at least 2 times in random sequence. Every 2.7 seconds a measurement is recorded 150 measurements were taken per air velocity. The steady state is also verified afterwards by considering the moving average of the temperatures. During a series of measurements the set point of the water temperature is not changed (reference set point at 70°C). Only the air mass flow rate is changed in small steps (6 measurements per series). A number of tests were performed at both higher and lower water temperatures (50°C, 60°C, 80°C) and with higher water mass flow rate to verify the measurement at reference temperature. All other water temperature measurements are within the accuracy of the measurement. Only the reference measurement (70°C) will be used to report.

Based on the geometry of the heat exchanger, the temperature gradient in a horizontal plane at the end of the test section is expected to be constant. This was confirmed using an infra red (IR) camera (see Figure 5). Therefore a single row of 9 thermocouples was mounted vertically across the test section. The thermocouples were spaced equidistantly (see Figure 6, (3)). These obtained values are used to compute the area-averaged temperatures, to be used in further calculations. The IR camera is from Dias Infrared Systems (type Midas 320L), with a conservatively estimated accuracy of 1°C (if calibrated). The IR camera has a resolution of 320x240 pixels and is used to verify the thermocouple measurements and the temperature distributions. IR measurements require a good calibration and a careful setting up of the experiment. For example one must avoid reflections from walls, nearby setups etc., as these influence the measurements. Next, a correct surface emissivity value is required to determine the temperature from the acquired radiation. In preparing of this experiment we therefore considered the three recommendations of the ASTM standards. The main reflections in the measurements were due to the walls of the test section downstream of the heat exchanger. To remove these, we decided to place a thin slice of metal foam at the test section exit. This material also has a rather high constant emissivity due to its homogenous nature, allowing for proper IR measurements. That emissivity was found to be 0.82 using a calibrated thermocouple attached to the metal foam. The thermocouple is made visible on the IR image by adding a small piece of aluminium foil around it, so that in the post-processing of the IR images (using Matlab and GORATEC), the thermocouple is visible as a 9 pixels square. At the start of the measurements with the IR camera, more thermocouples are placed along the metal foam to check the uniformity of the emissivity. The complete test setup to measure the outlet air temperature is shown in Figure 6.

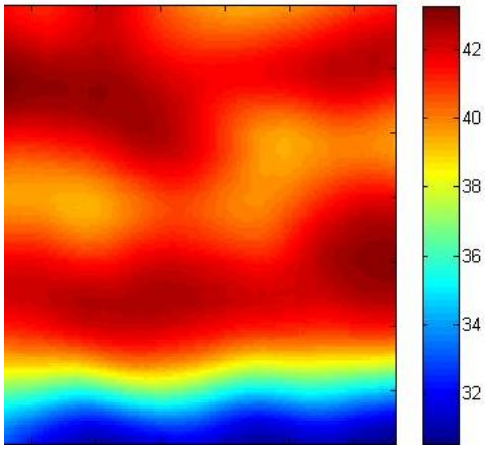

Figure 5 IR image of test section (in °C) at $\dot{m}_{air}$ = 0.26 kg/s; The capture is filtered in Matlab®.

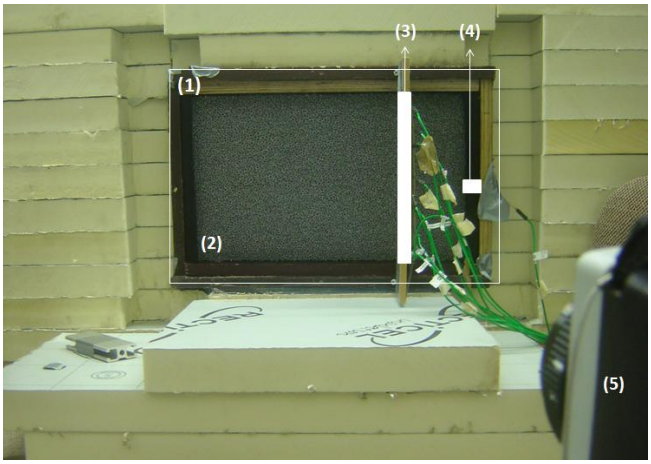

Figure 6 Photo of the insulated test section (1); external placed metal foam (2); vertical temperature reading (3); thermocouple for determination and verification of the foam's emissivity (4) and the IR camera (5)

The averaged air temperature based on the 9 thermocouples is compared to the IR measurement, and these showed a good agreement (Table 2). Next to the closed heat balance within 3%, this confirms the fact of accurate air outlet temperatures. The thermocouple-based averaged temperatures are used in further calculations.

Measurements at 70°C water temperature; with the louvered fin heat exchanger		
$\dot{m}_{air}$ **(in kg/s)**	thermocouples (in °C)	IR capture (in °C)
$\mathbf{0.204 \pm 0.01}$	42.06 ± 0.1	42.4 ± 1
$\mathbf{0.256 \pm 0.014}$	39.74 ± 0.1	39.64 ± 1
$\mathbf{0.309 \pm 0.018}$	38.62 ± 0.1	38.95 ± 1
$\mathbf{0.36 \pm 0.02}$	37.84 ± 0.1	37.2 ± 1

Table 2 Measurements of the IR camera.

To ensure the quality of the measurements an extensive error propagation is made. The uncertainties on the calculated results were determined with the root-sum-square method. The uncertainties on the thermodynamic properties of water are calculated according to the The International Association for the Properties of Water and Steam (IAPWS IF-97). The uncertainties on the density of the air are calculated using the ideal gas law. Standard error propagation rules as described by Moffat [13] were used to determine the total uncertainty. For the louvered fin heat exchanger, the relative uncertainty on $\dot{m}_{air}$ ranges from 4.4% to 6.0%; on $\dot{Q}_{average}$ ranges around 1%; on $R_{overall}$ from 5.4% to 5.7% (with the *LMTD* method); on R^*_{ext} from 6.8% to 8.3%; on $\Delta p_{air,HX}$ from 1.5% to 4.5%; on the friction factor from 9.6% to 12.1% and on PEC from 11.9% to 15.0%. For the metal foam heat exchanger, the relative uncertainty on $\dot{m}_{air}$ ranges from 4.5% to 5.8%; on $\dot{Q}_{average}$ ranged from 0.6% to 2.2% ; on $\Delta p_{air,valve}$ ranges from 3.4% to 5.2% ; on $R_{overall}$ from 5.16% to 5.6% (with the *LMTD* method); on R^*_{ext} from 6.5% to 7.6%; on $\Delta p_{air,HX}$ from 1.5% to 20.6% (high uncertainties in low velocity range $\approx 1 m/s$); on the friction factor from 10.4% to 15.5% and on PEC from 11.9% to 16.5% (with an average of 13.3%).

COMPARISON OF BOTH HEAT EXCHANGERS

For the determination of the friction factor (Eq. (14)), the minimal flow area A_c in case of the metal foam heat exchanger is calculated by subtracting the heat transferring surface (for the first tube row in the flow direction) from the total flow area and multiply this with the foam's porosity. The surface-to-volume ratio of 440m²/m³ for this in-house manufactured 10 PPI metal foam is reported in De Jaeger et al. [3], with an uncertainty of 8%. The total surface area A_0 is thus determined by multiplying this specific surface area with the metal foam volume. Furthermore G_c is calculated through Eq. (15) and (16). For the louvered fins, Eq. (14) is determined by following Wang et al. [14]. Both friction factors were plotted in function of the mass flow rate in Figure 7.

$$V_{max} = \frac{A_{HX}}{A_c} v_{air} \quad (15)$$

$$G_c = \rho_{air} * V_{max} \quad (16)$$

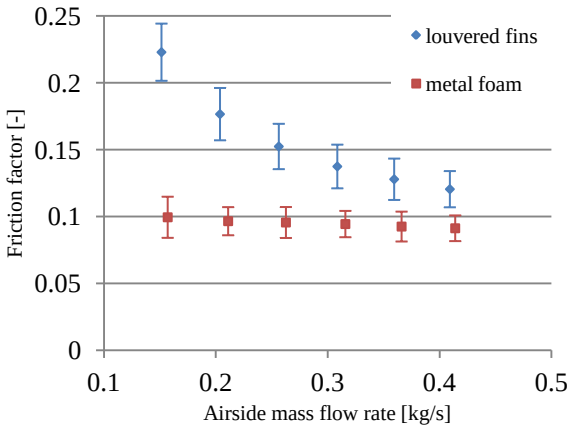

Figure 7 Kays and London friction factor in function of the airside mass flow rate

The friction factor of the louvered fin heat exchanger is surprisingly higher than of the metal foam heat exchanger. The friction factors correspond to a pressure drop of respectively 23.9 Pa to 94.5 Pa for the louvered fins and 9.7 Pa to 62.1 Pa for the foam. However, if we consider Fig. 4, we can see that the 10 PPI metal foam structure is more 'open' than the densely packed louvered fins (fin pitch: 1.4 mm). Remarkably, the friction factor of the metal foam heat exchanger is relatively flat. This is caused by the highly unsteady flow regime occurring within the foam. In laminar flow regime a von Kármán street (unsteady-oscillating) will be induced, whereas for turbulent regime more unsteady vortices will be induced. For this study, the Reynolds number based on the strut diameter and the interfacial velocity ($\frac{\rho\, d_f\, v_i}{\mu}$) ranges from 69.09 to 182.05. The interfacial velocity is calculated as the Darcy velocity, Eq. (17), on the porosity. The strut diameter is calculated from the measured strut cross sectional area in the middle of the strut. According to experiments by Seguin et al. [15-16] on porous media, laminar regime end at a pore Reynolds number of 180, whereas a value of 900 corresponds to a stabilization of the vortex velocity gradient fluctuating rate. As a pore Reynolds number of 1256 corresponds in the case of 10 PPI foam with a strut Reynolds number of 69.66, the regime in this study can be considered highly unsteady. This results in a flat friction profile. This limits further improvements to decrease the friction factor at higher velocities. This phenomenon is also experienced with the louvered fin heat exchanger: at higher mass flow rates (> 0.4 kg/s) the friction factor is also flatting through the unsteady vortices creation.

$$v_{Darcy} = \frac{\dot{m}}{\rho\, A_{HX}} \tag{17}$$

As the required pumping power is lower for the metal foam heat exchanger, the airside resistance R^*_{ext} is significantly higher. This is related to the lower available heat transfer area of the foam structure. The used metal foam has a heat transferring surface of 1.016 m², calculated with the measured surface-to-volume ratio in [3]. This is only 66% of the heat transferring surface of the current state-of-the-art louvered fin heat exchanger (1.544 m²). The trend of both series is very similar. For both units the airside heat transfer resistance is the dominating component, accounting up to 92% of the total resistance.

The PEC is plotted in Fig. 8, and as can be seen, the performance of the louvered fins is better at higher velocity. There is less difference at lower velocities (24% when comparing the average values). For an air velocity of 3.1 m/s the difference in performance is 59%. The reason for this evolution is related to the stepper decline of the airside resistance and the friction factor for the louvered fin heat exchanger.

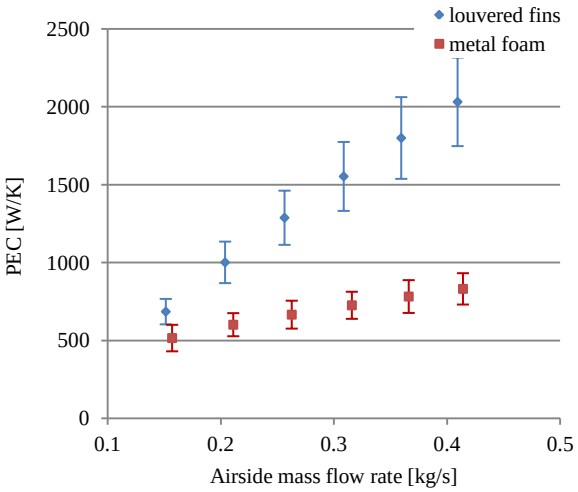

Figure 8 The performance factor PEC in function of the airside mass flow rate

To increase the performance of the metal foam heat exchanger, one can consider using other foam types. For example, a 20 PPI foam heat exchanger ($\varepsilon = 0.937$; $\sigma = 720\, m^2/m^3$ [3]) will have a higher heat transfer surface (1.66m²) which is very comparable to that of the louvered fin unit. This 20 PPI foam could not be used in this study, as it is not yet been able to make 20 PPI in-house with a thickness of 24mm, in order to make an exact replica of the louvered fin heat exchanger. However in the future we will be able to obtain a 24mm thick polyurethane preform.

This denser foam will result in a similar increase in the pressure drop. So changing the foam type might improve the situation, but considering the big differences especially at high velocities, additional measures will be required to make the metal foam more competitive. One of the most important considerations will be the thermal contact resistance.

INFLUENCE OF THE CONTACT RESISTANCE

It is difficult to measure the contact resistance, because of the high thermal conductivity of the material, which results in very low temperature jumps across the interface. Several authors are simply neglecting the interface contact resistance contribution to R^*_{ext} [17]. Other authors like Jamin et al. [18] tried to minimize the influence of the contact resistance by applying thermal grease (e.g. DOW340) to the interface. Bonding the foam is a difficult task because of the high porosity, which is otherwise an advantage. It results in many small spot-contacts instead of the typical line-contacts. ElSherbini and Jacobi [19] investigated the thermal contact resistance in a plain fin-and-tube evaporator, comparing units with a fin collar to those without. The authors reported a significant contact resistance contribution, which could be reduced by 50% when using collars. By consequence, most fin-and-tube heat exchangers are equipped with collars, including the used coil. Elsherbini and Jacobi [19] reported a thermal contact resistance of 9.44 kW m^{-2} K^{-1} (press-fit) for a louvered fin heat exchanger with collar. The fin collars completely overlap the tubes, which results in a contact resistance of 6.108

10^{-4} K/W. With increasing air mass flow rate, this represents a relative contribution of the contact resistance to the overall thermal resistance ranging from 7.7% to 11.1%. This is in good agreement with the work of Kim et al. [20] and Jeong et al. [21]. They study the contact resistance in units similar to the louvered fin heat exchanger considered here (with 7 mm tubes), and reported values as high as 15% of the overall thermal resistance. Because of the many small spot-contacts, the pressed-fitted metal foam heat exchanger is expected to have even higher contributions.

We explore the impact of the contact resistance of the foam heat exchanger through a paper of De Jaeger et al. [22]. The authors have investigated the thermal contact resistance for four different bonding methods by minimizing the difference between the calculated heat transfer via a zeroth order model and experimental data. By varying pore size, porosity, aluminium alloy, foam height, air mass flow rate, air inlet temperature and bonding method, it is seen that only the last variable causes a largest impact on the contact resistance. The authors used the same metal foams as in this paper. The resulting contact resistance is 1.84 10^{-3} m²K/W for press-fit bonding. All values with a conservative uncertainty of 11.4%. Based on this value, the contact resistance is evaluated to be 0.011 K/W; which results in a contribution of the contact resistance to the overall resistance ranging from 47.9% to 68.4% for varying airside velocity. This is comparable with the finding of T'Joen et al. [11] and Sadeghi et al. [23]. The last authors have experimentally measured the thermal contact resistance of a metal foam heat sink in a vacuum test chamber, by measuring the power of the heater and the temperatures of the heat sink. The authors tested four metal foams with different porosities (0.903 to 0.952) and PPI-values (10 and 20), by varying the compression load on the metal foam. It is clear that increasing the load, decreases the contact resistance because the contact surface area increases. Relative contact resistance contributions were measured up to 58% of the overall resistance. T'Joen et al. [11] considered the case of metal foam covered tubes. Metal foam is fixed to the tube by epoxy glue. Through destructive testing the thickness of the epoxy could be measured and was taken conservatively on 0.3mm. By modelling the epoxy layer as a cylinder surrounding the tube, the contact resistance can be calculated. Very high relative contributions are found: varying between 6% and 55% of the overall resistance.

By plotting R_{ext} for both heat exchangers as a function of the airside mass flow rate, the convective resistance of the metal foam actually is lower than that of the louvered fin heat exchanger at higher air velocities (see Fig. 9). The convective resistances cross at an airside velocity of 2.75 m/s. This means that from that point on, the convection coefficient is higher in the foam heat exchanger. But, due to the high contact resistance, the metal foam heat exchanger has a lower overall heat transferring performance ($\dot{Q}_{average}$). This highlights that the contact resistance is in fact the major problem for foam heat exchangers. However if we also consider the uncertainty on R_{ext} no conclusions can be taken, because the uncertainties for the foam heat exchanger are high. The maximum relative uncertainty on R_{ext} is 44.9% (for the highest air velocity set point). This high uncertainty is caused by the strong influence of the uncertainty on the contact resistance.

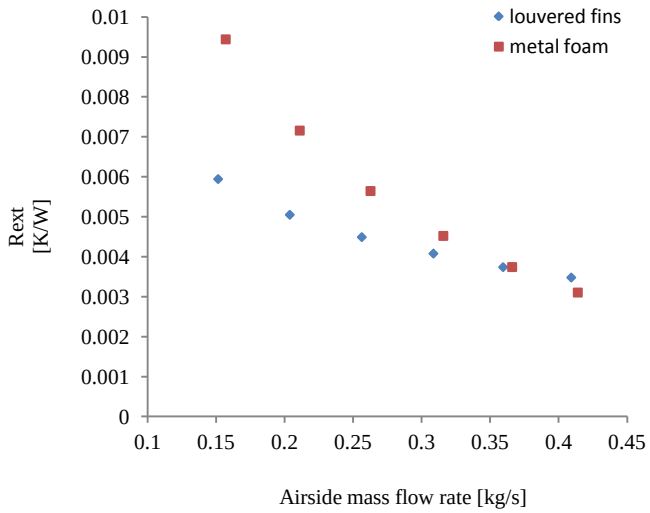

Figure 9 The external convective resistance in function of the airside mass flow rate

CONCLUSIONS

In this study, the performance of an open-cell aluminium foam heat exchanger and an adapted inclined louvered fin heat exchanger is compared in a wind tunnel experiment. The following conclusions were drawn:

- It was found that the required pumping power for the metal foam heat exchanger is lower than for his louvered fin counterpart. Furthermore, there is observed that the friction factor flattens-out through the induced highly unsteady flow in the foam, even at low velocities (1.1m/s). This limits further improvements for decreasing the friction factor at higher velocities.
- According to the predefined PEC, taken as the ratio of the thermal conductance to friction factor, the current state-of-the-art louvered fin heat exchanger outperforms the metal foam one. However, at low velocities (<1.5 m/s) this difference is acceptable. Furthermore, foam has other added values that have to be taken into account: e.g. weight, shape-ability, etc.
- The contribution of the thermal contact resistance to the overall thermal resistance is experienced to be very high for the metal foam heat exchanger. However, this resistance is often neglected or lumped with the airside resistance, even in foam applications. Contributions up to 58% of the overall thermal resistance were calculated. Whereas the louvered fin heat exchanger, with collared fins, only experience a contribution up to 11.1%.

Previous bullets show the necessity to optimize the foam heat exchanger (which was a prototype in this study). Future work will involve:

- An improved contact technology (e.g. brazing or epoxy bonding)
- Higher PPI value: 20 PPI foam will already give a higher heat transfer surface in comparison with the louvered fin heat exchanger.

ACKNOWLEDGEMENTS

The authors want to express gratitude to Bekaert for the close cooperation and financial support. They also want to thank Robert Gilles and Patrick De Pue for the technical support.

REFERENCES

[1] Bressand F., Farrell D., Hass P., Morin F., Nyquist S., Remes J., Roemer S., Rogers M., Rosenfeld J. and Woetzel J., Curbing global energy-demand growth: The energy productivity opportunity, McKinsey, McKinsey&company, San Francisco, 2007, pp. 48

[2] He J., Liu L. and Jacobi A.M., Air-side heat-transfer enchancement by a new winglet-type vortex generator array in a plain-fin round-tube heat exchanger, Journal of Heat Transfer, Vol. 132, July 2010, pp. 071801-1 - 071801-9.

[3] De Jaeger P., T'Joen C., Huisseune H., Ameel B. and De Paepe M., An experimental validated and parameterized periodic unit-cell reconstruction of open-cell foams, Journal of Applied Physics, Vol. 109, 2011, pp. 103519-1 – 103519-10.

[4] Lu T.J., Valdevit L. and Evans A.G., Active cooling by metallic sandwich structures with periodic cores, Progress in Materials Science, vol. 50, 2005, pp. 789-815.

[5] Shah R. K. and Sekulic Dusan P., Fundamentals of heat exchanger design, 2003, Print ISBN: 9780471321712, published by Wiley.

[6] Sertkaya A.A., Altinisik K. and Dincer K., Experimental investigation of thermal performance of aluminum finned heat exchangers and open-cell aluminium foam heat exchangers, Experimental Thermal and Fluid Science, vol. 36, 2012, pp. 86-92.

[7] T'Joen C., Steeman H.-J., Willockx A. and De Paepe M., Determination of heat transfer and friction characteristics of an adapted inclined louvered fin, Experimental Thermal and Fluid Science, vol. 30, 2006, pp. 319-327.

[8] Huisseune H., T'Joen C., Brodeoux P., Debaets S. and De Paepe M., Thermal hydraulic study of a single row heat exchanger with helically finned tubes, Journal of Heat transfer, vol. 132, 2010, pp. 061801-1 - 061801-8.

[9] Huisseune H., Performance evalution of louvered fin compact heat exchangers with vortex generators, PhD thesis, Ghent University, Ghent, Belgium. Promotor: De Paepe M, 2011.

[10] Park Y.-G., Rational approaches for combining redundant, independent measurements to minimize combined experimental uncertainty, Experimental Thermal and Fluid Science, vol. 34, 2010, p. 720-724.

[11] T'Joen C., De Jaeger P., Huisseune H., Van Herzeele S., Vorst N. and De Paepe M., Thermo-hydraulic study of a single row heat exchanger consisting of metal foam covered round tubes, International Journal of Heat and Mass Transfer, vol. 53, 2010, pp. 3262-3274.

[12] Liu P.S., A new method for calculation the specific surface area of porous metal foams, Philosophical Magazine Letters, vol. 90, 2010, pp. 447-453.

[13] Moffat R. J., Eaton J.K. and Onstad A., A method for determining the heat transfer properties of foam-fins, Journal of Heat transfer, vol. 131, 2009, pp. 011603-1 - 011603-7.

[14] Wang C.-C., Lee C.-J., Chang C.-T., Lin S.-P., Heat transfer and friction correlation for compact louvered fin-and-tube heat exchangers, International Journal of Heat and Mass Transfer, vol. 42, 1999, pp. 1945-1956.

[15] Seguin D., Montillet A. and Comiti J., Experimental characterisation of flow regimes in various porous media – I: limit of laminar flow regime, Chemical Engineering Science, vol. 53, nr. 21, 1998, pp. 3751-3761.

[16] Seguin D., Montillet A., Comiti J. and Huet F., Experimental characterisation of flow regimes in various porous media – II: transition to turbulent regime, Chemical Engineering Science, vol. 53, nr. 22, 1998, pp. 3897-3909.

[17] Du Y.P., Qu Z.G., Zhao C.Y., Tao W.Q., Numerical study of conjugated heat transfer in metal foam filled douple-pipe, International journal of heat and mass transfer, vol. 53, 2010, pp. 4899-4907.

[18] Jamin Y. L. and Mohamad A.A., Enhanced heat transfer using porous carbon foam in cross flow – Part I: forced convection, Journal of Heat Transfer, vol. 129, June 2007, pp. 735-743.

[19] ElSherbini A.I., Jacobi A.M. and Hrnjak P.S., Experimental investigation of thermal contact resistance in plain-fin-and-tube evaporators with collarless fins, International Journal of Refrigeration, vol. 26, 2003, pp. 527-536.

[20] Kim C. N., Jeong J. and Youn B., Evaluation of thermal contact conductance using a new experimental-numerical method in fin-tube heat exchangers, International Journal of Refrigeration, vol. 26, 2003, pp. 900-908.

[21] Leong J., Kim C. N. and Youn B., A study on the thermal contact conductance in fin-tube heat exchangers with 7 mm tube, Technical Note, International Journal of Heat and Mass Transfer, vol. 49, 2006, pp. 1547-1555.

[22] De Jaeger P., T'Joen C., Huisseune H. and De Paepe M., On the thermal resistance of open-cell aluminum foam, Journal of heat and mass transfer, *preprint summited to the journal*, 2012.

[23] Sadeghi E., Hsieh S. and Bahrami M., Thermal conductivity and contact resistance of metal foams, Journal of Physics D: Applied Physics, vol. 44, 2011, pp. 125406 (7pp).